ELSEVIER

Journal of Molecular Catalysis A: Chemical 98 (1995) 123–133

JOURNAL OF MOLECULAR CATALYSIS A: CHEMICAL

Linear low density polyethylene: catalyst system effect on polymer microstructure

Giulio Balbontin [a], Isabella Camurati [a], Tiziano Dall'Occo [a,*], Robert C. Zeigler [b]

[a] *Himont Italia, 'Centro Ricerche G. Natta', P. le Donegani 12, 44100 Ferrara, Italy*

[b] *Himont USA Inc., Research and Development Center, 912 Appleton Road, Elkton, MD 21921, USA*

Received 20 July 1994; accepted 23 January 1995

Abstract

The microstructure in terms of molecular mass distribution (MMD) and chemical comonomer distribution (CCD) of linear low density polyethylene (LLDPE) is greatly influenced by the catalytic system and process conditions. Furthermore, the 1-olefin insertion in the polymer chain can be distinguished between intramolecular and intermolecular distribution. To investigate the intermolecular CCD and the MMD, four LLDPEs (ethylene–1-butene copolymers) from different catalytic systems based on $Ti/MgCl_2$ catalysts, a zirconocene complex and a vanadium compound, are studied. The microstructure of the whole polymers and of their fractions are examined by size exclusion chromatography (SEC), differential scanning calorimetry (DSC), and ^{13}C NMR analysis. Further information about CCD is also obtained by DSC analysis on the whole samples by applying a particular thermal treatment, named thermal fractionated crystallization (TFC), based on isothermal crystallization of the polymers from the melt at fixed temperatures. The results obtained with the different analytical techniques show that the examined polymers have a very distinct microstructure depending on the catalyst type.

Keywords: ^{13}C NMR analysis; Calorimetry; Differential scanning calorimetry analysis; Fractionation; Linear low density polyethylene; Polyethylene; Polymer microstructure; Size exclusion chromatography analysis; Thermal fractionated crystallization

1. Introduction

Linear low density polyethylenes (LLDPE) are linear polyethylenes containing a small amount of short chain branching (SCB) along the chains due to the insertion of 1-olefin units during the polymerization reaction [1].

The polymer microstructure in terms of molecular mass distribution (MMD) and chemical comonomer distribution (CCD) greatly depends on the catalytic system and polymerization conditions [2–11]. It is reported that a great extent of polymerization active sites are present in heterogeneous catalytic systems [2–4,12] in comparison to homogeneous zirconocene-based catalysts [13]. This difference is responsible for the different MMDs [13] of the polymers, while only few works investigating the CCD of polymers from zirconocenes are published [14,15].

The 1-olefin insertion modes in polyethylene result both in intermolecular and intramolecular distribution heterogeneity. In the former case the 1-olefin can be homogeneously distributed along the single macromolecular chain, but each chain differs in composition from the other. In the latter case the 1-olefin is non-randomly distributed

* Corresponding author.

SSDI 1381-1169(95)00025-9

Table 1
LLDPE samples and molecular characterizations

LLDPE no.	Catalytic [a] system	Activity [b] kg/g-Mt/h	1-Butene [c] wt.-%	Density [d] g/cm^3	XSRT [e] wt.-%	$10^{-3} \cdot \bar{M}_w$ [f] g/mol	$\bar{M}_w/\bar{M}_n$	T_m [g] °C	ΔH_f J/g
1	Zr	186	6.0	0.9172	0.3	55.5	2.0	108	100
2	Mg–Ti(I)	241	8.0	0.9273	9.0	117.5	11.2	122	130
3	Mg–Ti(II)	38	7.5	0.9201	11.8	103.9	4.3	121	120
4	V	4	9.0	0.9093	2.0	323.1	3.3	96	103

[a] Zr = Zirconocene based system; Mg–Ti(I) = heterogeneous $MgCl_2$ supported Ti(IV) compound; Mg–Ti(II) = heterogeneous $MgCl_2$ supported Ti(III) compound; V = homogeneous vanadium based system.
[b] Polymerizations were performed in a 2.6 l stainless steel autoclave, see Experimental part.
[c] Calculated from ^{13}C NMR data.
[d] By density gradient column (ASTM D-1505).
[e] Weight percentage of polymer soluble in xylene at 25°C.
[f] By SEC.
[g] By DSC following the standard method.

along every chain. ^{13}C NMR analysis on fractions of LLDPE from a $SiO_2/TiCl_4$ catalytic system shows that the intramolecular distribution is essentially Bernoullian [2,12].

Another interesting topic is whether or not the CCD is related to the MMD. The analysis on cross-fractionated commercial LLDPEs [16] shows an inverse relationship between short chain branching content and molecular mass.

In order to investigate the microstructure of the polymers obtained from different catalytic systems, four samples of LLDPE (ethylene–1-butene) of similar chemical composition are prepared and their main characteristics are reported in Table 1. The polymers are fractionated by 'solution fractional crystallization' and analyzed by size exclusion chromatography (SEC), differential scanning calorimetry (DSC) and ^{13}C NMR.

Further information about CCD are also obtained by DSC analysis on the raw samples by applying a particular thermal treatment (thermal fractionated crystallization, TFC) [17]. This method is based on several steps of isothermal crystallization of the polymer on decreasing the temperature from the melt. This process favours the separation of the crystalline material in groups of lamellae having different thicknesses depending on the amount and distribution of the 1-olefin units in the macromolecular chains. In fact, according to the exclusion model [18], which describes the crystallite formation from copolymer chains comprised of units that can crystallize and units that cannot, the thickening of the polyethylene lamellae can be hindered by the presence of a 1-olefin unit at the chain folding. The fold period will thus depend on the frequency of not crystallizing units along the copolymer chains. The subsequent melting endotherm is made up of the same number of peaks as the isothermal crystallization steps. The area of the thermogram is proportional to the total amount of the crystalline part of the polymer, and the partial area between two fixed temperatures is proportional to the amount of crystalline material comprising lamellae of a specific size (the Thomson and Gibbs equation relates the lamella thickness to the melting temperature). Thus, by dividing the melting thermogram into 5 zones, it is possible to assign to each one an average SCB content (Table 2). These concepts are, in summary, depicted in Fig.

Table 2
Correlation between melting range and LLDPE composition [a]

Zone	A	B	C	D	E
Melting range (°C)	> 120	100–120	80–100	50–80	< 50
SCB [b] (CH_3/100C)	< 1.2	1.2–3.6	3.6–6.0	6.0–9.6	> 9.6

[a] Determined by DSC analysis (standard method) of narrow TREF fractions (SCB vs. T_m).
[b] By FT-IR at 1375 cm^{-1}.

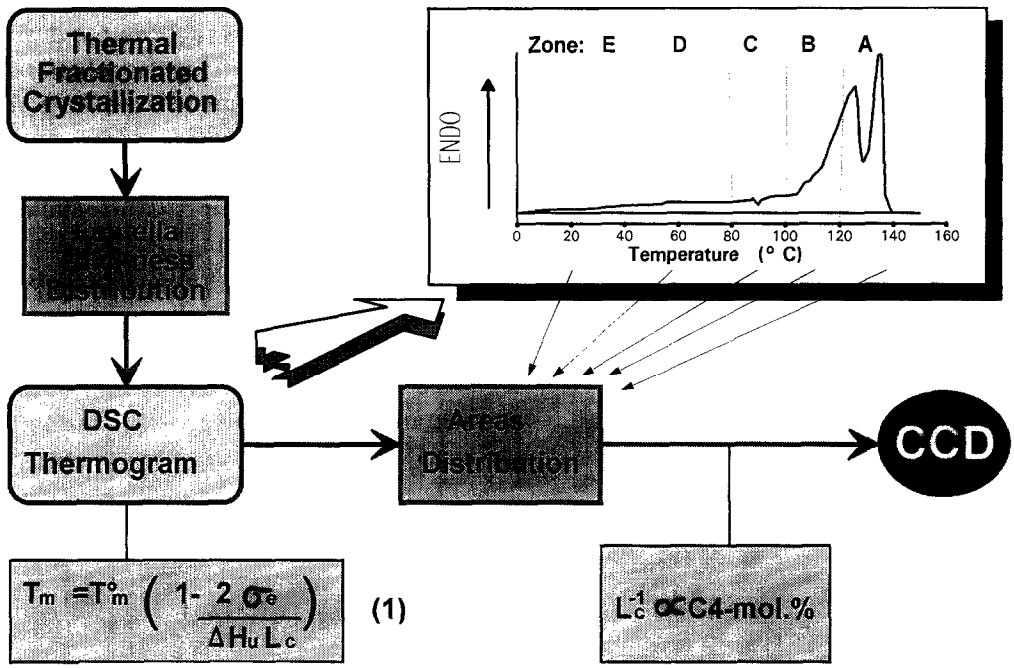

Fig. 1. Schematic representation of how to obtain the chemical comonomer distribution (CCD) through the thermal fractionated crystallization (TFC). Equation (1) is the Thomson and Gibbs relation where Lc is the lamella thickness; ΔH_u is the polyethylene molar heat of fusion; σ_e is the top and bottom specific surface free energy of the lamella; T_m° is the equilibrium melting temperature of HDPE; T_m is the melting temperature of the lamella of dimension Lc.

1. The distribution of the endotherm in zones permits the calculation of the areas 'A'–'E' (see Experimental and Table 5). and provides a semi-quantitative evaluation of the CCD.

2. Experimental

The polymers are synthesized on laboratory scale by using catalytic systems of different families, as reported in Table 1, in the best polymerization conditions.

2.1. Polymerization

Polymers 1–3 are obtained with the following procedure; propane (1.6 l), 1-butene, ethylene and hydrogen, in suitable amounts, are introduced into a thermostatically controlled 2.6 l stainless steel autoclave purified with an ethylene stream at 80°C. The polymerization temperatures are 50–75°C. Catalyst and aluminum alkyl are mixed in 10 ml of solvent (hexane or toluene), aged 5 min and added to the autoclave through a stainless steel vial with an ethylene overpressure. The total polymerization pressure is maintained constant by continuous feeding of ethylene/1-butene mixture. After degassing the monomers and propane, the polymer is isolated and dried in vacuum at 60°C.

The same procedure is applied to polymer 4 except that hexane is used instead of propane.

2.2. Fractionation

Preparative fractionation (solution fractionated crystallization) is performed by dissolving the polymers in xylene at 120°C in presence of 0.1 wt.-% of 2,6-di-t-butyl-*p*-cresol (BHT) and then cooling the solution to the collecting temperature of 55°C. After 1 h aging, the first soluble portion is collected. The same procedure is repeated for all the fractions at the temperatures 70, 80, 90 and 110°C.

2.3. Size exclusion chromatography (SEC)

The analysis are performed by using a WATERS 150-C GPC equipped with a TSK col-

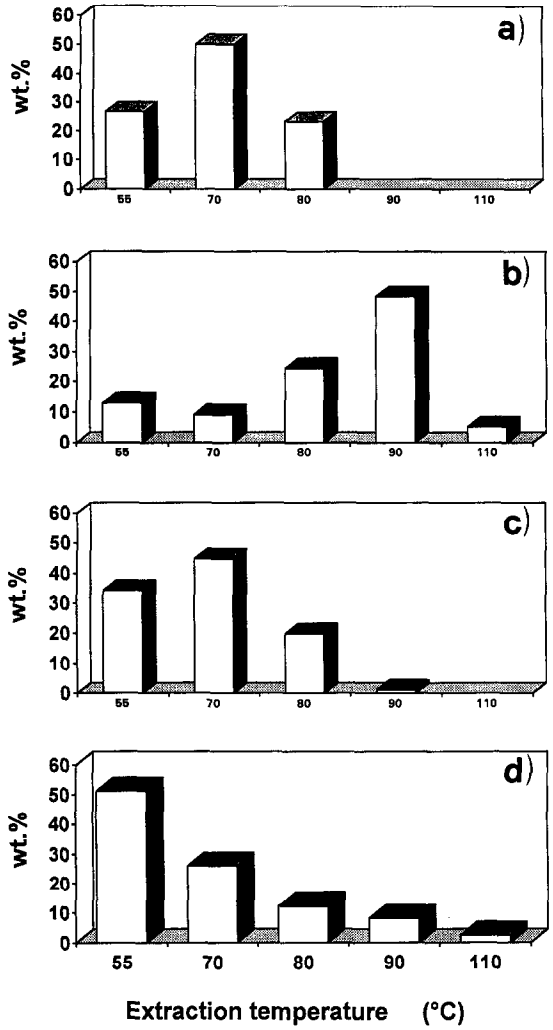

Fig. 2. LLDPE fractions distribution: a) LLDPE n1; b) LLDPE n2; c) LLDPE n3: d) LLDPE n4.

umn set (type GM-HT$_{xl}$), working at 135°C with 1,2-dichlorobenzene stabilized with 0.1 wt.-% of BHT. Monodisperse fractions are used as standard. The universal calibration is performed by using the Mark–Houwink constants calculated from those of polyethylene following the Scholte method [19].

2.4. ^{13}C NMR

The ^{13}C NMR spectra are recorded at 130°C on a Varian Unity-300 spectrometer operating at 75.4 MHz in the Fourier transform mode. About 6000 transients are accumulated for each spectrum with a 90° pulse and 12 s delay period between pulses. The sample solutions in 10 mm o.d. glass tubes are prepared by dissolving the polymer in 1,1,2,2-tetrachloro-1,2-dideuteroethane to give an 8% (wt./vol.) concentration.

The assignments are made according to Randall and Hsieh [20]. In our experimental conditions, the calculation according to their method gives an imprecise estimation of [BBB] and [BBE] triads because of the low 1-butene content. With the exception of fraction 1 of sample 2, which has a detectable amount of [BBB] triads, dyad distributions are determined by measuring the peak areas as individual peaks or small ranges.

The ethylene and 1-butene average sequence lengths n_e and n_b, are calculated according to the equations:

$$n_e = (2 \cdot [EE]/[EB]) + 1 \quad (2)$$

$$n_b = (2 \cdot [BB]/[EB]) + 1 \quad (3)$$

The monomer reactivity ratio product, $r_1 \cdot r_2$, is determined from the dyad distribution according to the equation:

$$r_1 \cdot r_2 = (4 \cdot [EE] \cdot [BB])/([EB] \cdot [EB]) \quad (4)$$

if: $r_1 \cdot r_2 > 1$, the polymer tends to a blocky structure; $r_1 \cdot r_2 = 1$, the structure is random; $r_1 \cdot r_2 = 0$, the comonomer units are isolated.

2.5. Standard DSC analysis

Calorimetric measurements are performed by using a differential scanning calorimeter Perkin Elmer DSC-7. The instrument is calibrated with indium and tin standards. Weighed samples (10 mg) are sealed into aluminum pans, heated to 180°C and kept at that temperature for long enough (4 min) to allow complete melting of all the crystallites; in this way any influence of the previous thermal history is removed. Then, after slow cooling at 10°C/min to 0°C, the samples are heated to 180°C at a rate of 10°C/min.

2.6. Thermal fractionated crystallization (TFC)

In order to achieve a fractionation of the polymer in terms of lamella size, the melted sample

(180°C) is cooled at nominal rate of 200°C/min to fixed crystallization temperatures of $T_{c1}=120$°C, $T_{c2}=100$°C, $T_{c3}=80$°C, $T_{c4}=50$°C and $T_{c5}=0$°C. An isothermal crystallization time of 120 min is chosen in order to achieve complete crystallization of the polymer fractions at the fixed temperature. Finally the sample is heated at 10°C/min to 180°C and the corresponding DSC curve is recorded. The thermogram curve, characterized by the same number of peaks as the isothermal crystallization temperatures, is then divided into five parts: area 'A', between 120°C and the end of the curve; area 'B', in the range 100–120°C; area 'C', in the range 80–100°C; area 'D', in the range 50–80°C; area 'E', below 50°C. Finally, by using the calculating program of DSC-7, the partial areas of the thermogram are calculated.

3. Results and discussion

3.1. Fractionation

Detailed information about the microstructure of polymers can be obtained only by analysing their fractions. Our method is substantially based on fractionation by crystallite size. In other words, polymer chains with increasing ethylene sequence length will be dissolved at higher temperature as is for TREF analysis [22].

In Fig. 2a–d and Table 3 are shown the fraction distributions of the four LLDPEs, and Fig. 3a and 3b display the SCB content and intrinsic viscosity (I.V.) as a function of the elution temperature, respectively.

Table 3
Fraction results and molecular mass of the whole polymers and their fractions

Sample	Extraction temperature	Fraction	SCB [a]	I.V. [b]	SEC molecular characteristic				
					$10^{-3}\cdot\bar{M}_n$	$10^{-3}\cdot\bar{M}_w$	$10^{-3}\cdot\bar{M}_z$	$\bar{M}_w/\bar{M}_n$	$\bar{M}_z/\bar{M}_w$
	°C	wt.-%	CH_3/100C	dl/g	g/mol	g/mol	g/mol		
1		100	1.4	2.0	55.4	112.1	196.5	2.0	1.8
1-1	55	26.6	2.0	2.1	34.9	111.6	200.3	3.2	1.8
1-2	70	50.0	1.6	2.0	63.1	131.1	221.0	2.1	1.7
1-3	80	23.1	1.3	2.1	59.4	124.4	219.6	2.1	1.8
1-4	90	0.3	–	–	–	–	–	–	–
2		100	1.8	1.9	10.7	119.6	488.2	11.1	4.1
2-1	55	12.9	5.9	0.8	7.0	35.0	148.6	5.0	4.2
2-2	70	9.1	2.3	1.2	10.5	69.7	311.4	6.6	4.5
2-3	80	24.5	1.1	2.2	25.8	201.6	734.2	7.8	3.6
2-4	90	48.3	0.4	2.4	44.4	189.5	670.4	4.3	3.5
2-5	110	5.1	0.3	2.4	57.1	173.1	531.7	3.0	3.1
3		100	1.9	1.5	24.0	103.9	297.7	4.3	2.9
3-1	55	34.3	3.5	1.6	16.1	105.4	320.3	6.5	3.0
3-2	70	44.7	1.0	1.8	31.0	109.8	395.2	3.5	3.6
3-3	80	19.9	0.6	1.8	23.6	107.6	335.4	4.6	3.1
3-4	90	1.1	–	1.9	36.7	115.0	321.1	3.1	2.8
4		100	2.3	3.4	99.2	323.9	1135.4	3.3	3.5
4-1	55	51.3	2.4	2.6	93.0	192.5	358.0	2.1	1.9
4-2	70	26.0	2.1	3.2	124.2	579.6	1601.9	4.7	2.8
4-3	80	12.1	1.4	5.7	74.6	532.8	1572.7	7.1	2.9
4-4	90	8.1	0.4	8.1	177.8	815.4	1938.4	4.6	2.4
4-5	110	2.5	–	–	–	–	–	–	–

[a] Short chain branching content by FT-IR at 1375 cm^{-1}.
[b] Intrinsic viscosity, measured in tetrahydronaphthalene at 135°C.

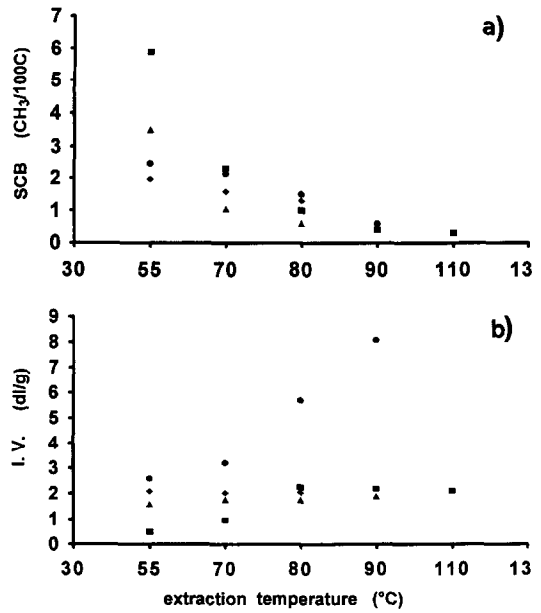

Fig. 3. Plot of the SCB content a) and the intrinsic viscosity (I.V.). b) vs. the fractionation temperature. SCB by FT-IR at 1375 cm^{-1}; (I.V.) measured in tetrahydronaphthalene at 135°C. ♦ LLDPE n1; ■ LLDPE n2; ▲ LLDPE n3; ● LLDPE n4.

Polymer 1 is separated into only three fractions; fraction 2, eluted at 70°C, is more than 50 wt.-% of the whole polymer. The SCB content slightly decreases (Fig. 3a) from fraction 1 to 3 while the molecular mass (as I.V.) (Fig. 3b) is almost constant, suggesting a separation by crystallite size. From these data it is possible to deduce that polymer 1 is homogeneous in composition.

Polymer 2 is distributed over all the five fractions (Fig. 2b). A remarkable amount of polymer soluble at a temperature higher than 90°C (fraction 4 and 5) is obtained, meaning that a low 1-butene insertion degree in the macromolecular chain occurs (Fig. 3a). Furthermore the SCB content greatly decreases from fraction 1 to 5, evidencing the heterogeneity of the comonomer distribution.

Polymer 3 shows a fractionation behaviour similar to polymer 1 with only a small amount of material soluble at a temperature higher than 90°C (Fig. 3c), but with a SCB distribution very similar to that of polymer 2 (Table 2). Again, as for polymer 2, fraction 1 displays the highest SCB content.

Polymer 4, which contains the highest 1-butene percentage and has the highest molecular mass (MM) (Table 1), shows a distribution of its fractions in the whole temperature range but with about the 80% of the polymer in the first two fractions. The SCB content slowly decreases on increasing the extraction temperature (fraction 1 to 3, Fig. 3a), while an increase of the MM is observed (Fig. 3b). This particular behaviour suggests that the separation occurred by MM instead of by crystallinity.

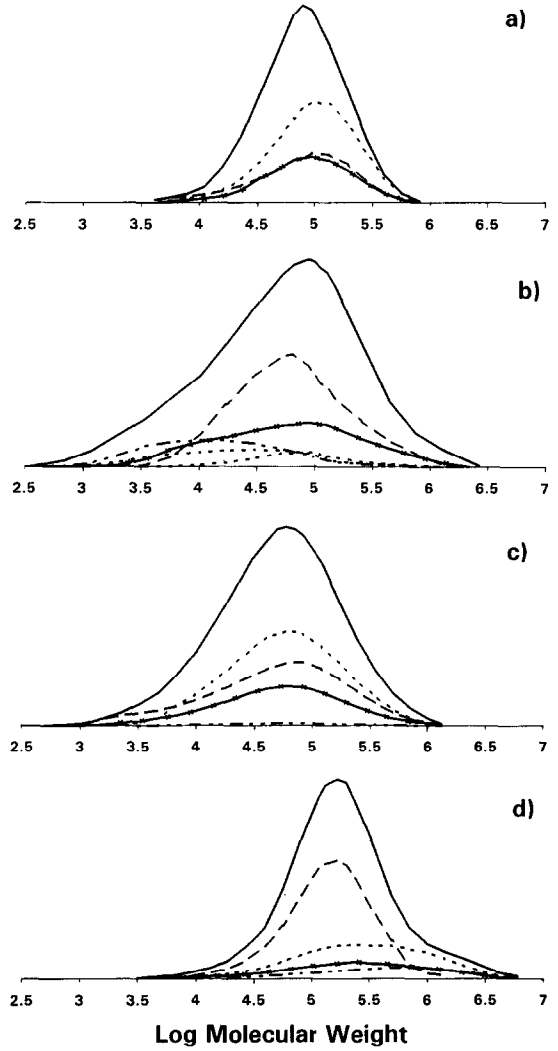

Fig. 4. SEC curves of the whole polymers and of their fractions: a) LLDPE n1; b) LLDPE n2; c) LLDPE n3: d) LLDPE n4. The SEC curves of the fractions are proportional to the fraction content. —— whole polymer, — — — fraction 1, - - - fraction 2, – × – × – fraction 3, — - — - fraction 4, — - - — fraction 5.

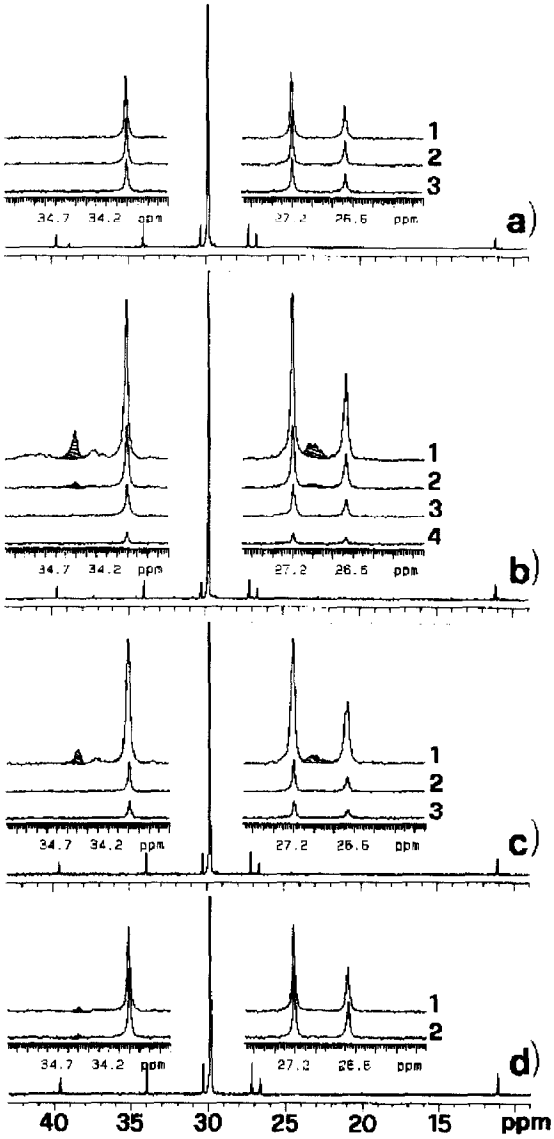

Fig. 5. ^{13}C NMR spectra of polymer 1–4 and magnifications of the 33–42 and 26–28 ppm regions of their fractions; a) LLDPE n1; b) LLDPE n2; c) LLDPE n3: d) LLDPE n4. Shaded peaks are due to the presence of 1-butene sequences.

In conclusion, from these data, it is possible to draw the following homogeneity order: LLDPE 1 > LLDPE 4 > LLDPE 3 > LLDPE 2.

3.2. Analysis on the fractions

It is recognized from literature that a narrow MMD can be obtained only if the catalytic system comprises a limited (better if it is a single) type of catalytic sites [23]. According to this hypothesis, it is also reasonable to expect a similar behaviour versus the comonomer reactivity, i.e. each catalytic site produces a polymeric chain with a particular composition. In order to throw some light on these concepts, SEC and ^{13}C NMR analysis on the fractions are performed.

3.3. SEC

The MM data are collected in Table 3 and represented in Fig. 4. A great difference between the polymers is observed.

Polymer 1, from homogeneous catalyst, shows the narrowest molecular mass distribution (MMD) typical of these systems [13]. Moreover, its fractions have the same molecular mass and MMD as the whole polymer.

Polymer 2 has the broadest MMD, higher than the typical polydispersity shown by Ti based systems ($\bar{M}_w/\bar{M}_n \approx 3$–6). Its fractions are narrower than the whole polymer and their MM increases in the order: fraction $1 < 2 < 3 \cong 4 \cong 5$ (see also Fig. 3b and Table 3).

Conversely, the SCB content decreases as already reported for commercial polymers [16].

Polymer 3 and its fractions have a symmetric MMD. From the analysis of the fractions, it is observed a decrease of SCB as for polymer 2 while the $\bar{M}_w$ remains practically constant.

Polymer 4, which has the highest 1-butene content as well as MM, displays an asymmetric MMD, characterized by a high MM tail. The fractions show different MM and MMD and, as for polymer 2, the SCB decreases as the MM increases. It is interesting to note that fractions 1 and 2, with similar SCB content, have very different MM (192000 and 579000 g/mol respectively) and MMD (Fig. 4d).

3.4. ^{13}C NMR

The spectra of the polymers together with the most interesting expanded region of all the fractions, are shown in Fig. 5. Dyad distribution, monomer average sequence length ($\bar{n}_e$ and $\bar{n}_b$) and $r_1 \cdot r_2$ are reported in Table 4.

Table 4
^{13}C NMR dyad distribution, and the calculated parameter of ethylene and 1-butene average sequence length and reactivity ratio product

Sample	Extraction temperature	Fraction	1-Butene	^{13}C NMR					
				Dyad distribution (mol.fraction)			Calculated parameters		
	°C	wt.-%	mol.-%	EE	EB	BB	$\bar{n}_b$	$\bar{n}_e$	$r_1 \cdot r_2$
1		100	3.1	0.940	0.060	0	1.00	32.3	–
1-1	55	26.6	4.1	0.921	0.079	0	1.00	24.3	0
1-2	70	50.0	3.0	0.943	0.057	0	1.00	34.1	0
1-3	80	23.1	2.2	0.957	0.043	0	–	45.5	[c]
1-4	90	0.3	–	–	–	–	–	–	–
2		100	4.2	0.907	0.088	0.005	1.11	21.6	–
2-1	55	12.9	13.5	0.763 [a]	0.204 [a]	0.033 [a]	1.32	8.5	2.42
2-2	70	9.1	4.7	0.910	0.086	0.004	1.09	22.2	1.97
2-3	80	24.5	2.1	0.967	0.033	0	–	59.6	[c]
2-4	90	48.3	0.7	0.986	0.014	0	–	141.9	[c]
2-5	110	5.1	–	–	–	–	–	–	–
3		100	3.9	0.925	0.073	0	1.00	26.3	–
3-1	55	34.3	7.9	0.848	0.147	0.005	1.07	12.5	0.78
3-2	70	44.7	1.8	0.962	0.038	0	–	51.6	[c]
3-3	80	19.9	1.2	0.976	0.024	0	–	82.3	[c]
3-4	90	1.1	–	–	–	–	–	–	–
4		100	4.7	0.905	0.095	0	1.00	20.0	–
4-1	55	51.3	5.4	0.895	0.104	0.001	1.02	18.2	<1
4-2	70	26.0	4.8	0.909	0.090	0.001	1.00	21.2	<1
4-3	80	12.1	2.8 [b]	–	–	–	–	–	–
4-4	90	8.1	0.8 [b]	–	–	–	–	–	–
4-5	110	2.5	–	–	–	–			

[a] Calculated from the triad distribution with the Randall method [20].
[b] By FTIR.
[c] Not calculated due to the undetectability of the [BB] dyad.

The results obtained show that polymer 1 is highly homogeneous. Its fractions have similar comonomer content and $\bar{n}_e$ values, while the 1-butene units are mainly isolated ([BB] = 0 and $r_1 \cdot r_2 = 0$).

Polymer 2 shows a broad chemical comonomer distribution. The fractions have a 1-butene content ranging from 13.5 mol% in fraction 1 to less than 1 mol% in fraction 4. Furthermore, fractions 1 and 2 show an appreciable content of [BB] sequences (see $\bar{n}_b$ value) and their $r_1 \cdot r_2$ (higher than 1) emphasize the blocky structure. As a consequence these fractions need more 1-olefin amount to be eluted at a fixed temperature (see Fig. 2a). The $\bar{n}_e$ values increase from fraction 1 to 4, becoming higher than 100, and approaching those of HDPE ($\bar{n}_e = \infty$) [21].

Polymer 3 has a 1-butene distribution and an ethylene sequence length distribution similar to polymer 2. However the $r_1 \cdot r_2$ value in fraction 1 is close to 1 as in nearly random copolymers.

Though 1-butene monomer inversions have been detected in LLDPE's [8] made with vanadium-based catalysts, no inversions are detected in polymer 4, probably due to the low 1-butene content and low [BB] dyad sequence level. The $\bar{n}_b$ and $\bar{n}_e$ values of the first two fractions are comparable within the experimental error. A precise evaluation of these parameters for the remaining fractions is difficult to obtain because of the low 1-butene content. Considering that about the 80 wt.-% of the whole polymer is composed of the fractions 1 and 2, it is reasonable to consider polymer 4 homogeneous in CCD.

Table 5
Partial area distribution of DSC–TFC thermograms of the whole samples and their fractions

Sample	Extraction temperature	Fraction	1-Butene	DSC–TFC		DSC–TFC partial area distribution				
				T_m [a]	ΔH_f [b]	Area 'A' >120°C	Area 'B' 100–120°C	Area 'C' 80–100°C	Area 'D' 50–80°C	Area 'E' <50°C
	°C	wt.-%	mol.-%	°C	J/g	%	%	%	%	%
1	–	100	3.1	114	123	–	54.3	24.5	15.1	6.1
1-1	55	26.6	4.1	110	123	–	35.0	35.7	18.7	10.6
1-2	70	50.0	3.0	112	109	–	57.2	30.1	12.3	–
1-3	80	23.1	2.2	114	122	–	70.0	20.3	9.7	–
1-4	90	0.3	–	115	126	0.1	62.8	20.0	17.2	–
2	–	100	4.2	132	183	50.8	25.0	7.7	9.0	7.4
2-1	55	12.9	13.5	100	62	–	18.7	35.6	33.3	12.4
2-2	70	9.1	4.7	116	132	1.2	57.6	21.6	14.7	4.8
2-3	80	24.5	2.1	120	133	16.3	62.6	14.7	6.4	–
2-4	904	8.3	0.7	128	162	68.6	24.5	5.5	1.3	–
2-5	110	5.1	–	136	183	78.5	16.4	4.1	1.0	–
3	–	100	3.9	123	120	33.8	37.4	16.9	10.5	1.4
3-1	55	34.3	7.9	99	122	0.7	15.4	26.3	28.3	29.3
3-2	70	44.7	1.8	128	146	33.2	45.1	14.3	7.4	–
3-3	80	19.9	1.2	123	165	44.8	38.7	9.8	6.8	–
3-4	90	1.1	–	131	173	64.3	25.9	6.4	3.4	–
4	–	100	4.7	98	93	0.8	21.9	46.8	19.7	10.8
4-1	55	51.3	5.4	97	90	–	2.6	56.4	24.6	16.5
4-2	70	26.0	4.8	103	94	–	24.3	38.8	21.2	15.4
4-3	80	12.1	2.8	114	101	–	54.2	28.6	17.3	–
4-4	90	8.1	0.8	135	121	62.0	21.7	7.7	8.6	–
4-5	110	2.5	–	134	90	67.4	19.4	7.5	5.7	–

[a] Of the main peak.
[b] Total fusion enthalpy.

3.5. DSC – thermal fractionated crystallization (TFC)

The use of the DSC after the TFC treatment provides qualitative information about the ethylene sequence length and their distribution in the macromolecular chains [17].

In Table 5 and Fig. 6 are shown the data and the endotherms, after TFC treatment, of the four polymers and their fractions.

The fractions of polymer 1 melt almost in the same range of the whole sample and show melting curves with similar shape. Furthermore, about 50% of the polymer and of the fractions melt in the range of temperature defining the zone 'B' to which corresponds a SCB content (Table 2) between 1.2–3.6 CH_3/100C. The same results are also found by IR analysis (Table 3).

Moreover, ^{13}C NMR data agree with the fact that the 1-butene is equally distributed in all the fractions.

Polymer 2 shows the broadest melting curve covering the range between the zones A–E; its fractions melt in different ranges of temperatures with different SCB content and have narrower endotherms. This reflects the efficiency of the fractionation according to crystallite size (Fig. 5b). The whole polymer has about 50% of the

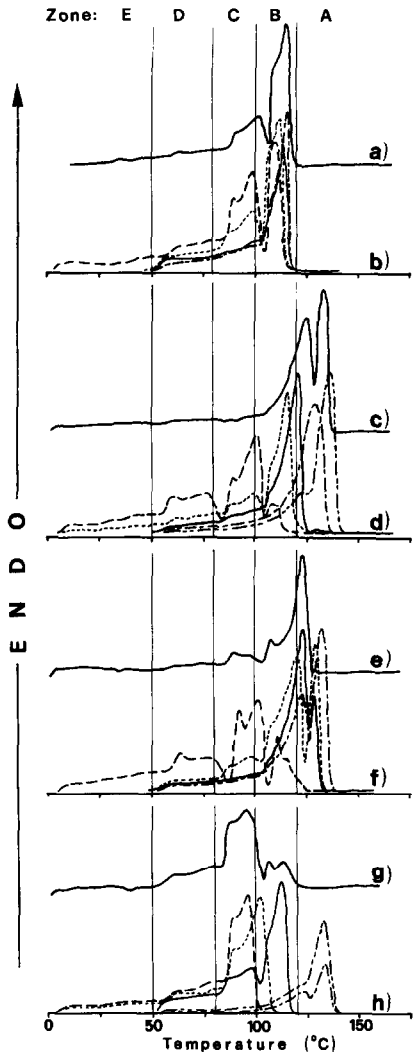

Fig. 6. DSC thermograms of the whole polymers and their fractions after TFC treatment: a) polymer 1; b) fractions 1–4 of polymer 1; c) polymer 2; d) fractions 1–5 of polymer 2; e) polymer 3; f) fractions 1–4 of polymer 3; g) polymer 4; h) fractions 1–5 of polymer 4; — — — fraction 1, - - - fraction 2, —— fraction 3, — - — - fraction 4, — - - — fraction 5.

endotherm in the range of the zone 'A' to which is related the melting of scarcely modified macromolecules (SCB content < 1.2 CH_3/100C).

For polymer 3, area 'B' is higher than area 'A' in spite of a lower 1-butene content than polymer 2 (Table 5). Again, the thermograms of the fractions evidenced a distribution intermediate between polymers 1 and 2 but closer to polymer 2.

Polymer 4 has a considerable melting-heat in the range of temperature defining zones 'B', 'C' and 'D', like polymer 1. Fractions 4 and 5, composed of poorly modified PE chains, do not contribute significantly to the endotherm of the whole polymer because of their small amount.

4. Conclusion

The evaluation of the chemical composition distribution from DSC data (after TFC) on the whole polymers are in good agreement with data from ^{13}C NMR and IR analysis on the polymer fractions.

The four catalytic systems produce polymers with different microstructure regarding MM and 1-butene insertion.

Homogeneous catalysts give a good distribution of the comonomer in all the fractions: both polymer 1 and 4 show a constant value of the average ethylene sequence length in all the fractions and the $r_1 \cdot r_2$ value is close to 0 or much less than 1. Furthermore, the narrow MMD of polymer 1 may suggest that a single family of catalytic sites or more than one, but with the same k_p/k_{tr} (where k_p and k_{tr} are the kinetic polymerization and transfer constants, respectively) are effective.

The same consideration applies to polymer 4 taking into account that a great extent of the whole polymer is in fraction 1. Fraction 2 differs only in MM and MMD. Thus it should be stressed that polymer 4 has a narrow CCD independent of the fact that MMD of the fractions is not homogeneous.

Polymers with different characteristics are obtained from heterogeneous catalysts, in fact the broad MMD and CCD observed could be explained by hypothesizing more families of active sites [3] having different reactivity toward comonomer and different sensitivity to hydrogen as MM regulator. The ^{13}C NMR analysis on fraction of polymer 2 shows in addition to the different comonomer content a tendency to a blocky structure as deduced from the $r_1 \cdot r_2$ value (Table 4).

It is worth noting that the MMD and CCD are two distinct characteristics of the polymer, independent from each other and related only to the

particular catalytic system. For example, polymers 1 and 4 show similar CCD but different MMD and polymers 2 and 3, both from heterogeneous $MgCl_2$ supported titanium catalysts, show different CCD and MMD.

References

[1] D.E. James, Encyclopedia of Polymer Science and Engineering, Vol. 6, Wiley Interscience, New York, 1986, p. 429.
[2] N. Kuroda, Y. Nishikitami, K. Matsuura and M. Miyoshi, Makromol. Chem., 188 (1987) 1897.
[3] M. Kakugo, T. Miytake and K. Mizunuma, Macromolecules, 24 (1991) 1469.
[4] T. Usami, Y. Gotoh and S. Takayama, Macromolecules, 19 (1986) 2722.
[5] V.A. Zakharov, L.G. Yechevskaya and G.D. Bukatov, Makromol. Chem., 190 (1989) 559.
[6] R. Spitz, V. Pasquet and J.F. Joly, Makromol. Chem., Macromol. Symp., 47 (1991) 95.
[7] T.A. Ojala and G. Fink, Makromol. Chem. Rapid Commun., 9 (1988) 85.
[8] N. Kuroda, Y. Nishikitani, K. Matsuura and N. Ikegami, Macromolecules, 25 (1992) 2820.
[9] W. Kaminsky and M. Schlobohm, Makromol. Chem., Macromol. Symp., 4 (1986) 103.
[10] R.G. Alamo and L. Mandelkern, Macromolecules, 22 (1989) 1273.
[11] L.D. Cady, Plast. Eng., January (1987) 25.
[12] H.N. Cheng, Polym. Bull., 23 (1990) 589.
[13] A. Ahlers and W. Kaminsky, Makromol. Chem., Rapid. Commun, 9 (1988) 457.
[14] R.G. Alamo and L. Mandelkern, Macromolecules, 22 (1989) 1273.
[15] K. Heiland and W. Kaminsky, Makromol. Chem., 193 (1992) 601.
[16] F.M. Mirabella and E.A. Ford, J. Polym. Sci.: Part B: Polym. Phys., 25, (1987) 777.
[17] G. Balbontin, I. Camurati, T. Dall'Occo, A. Finotti, R. Franzese and G. Vecellio, Angew. Makromol. Chem., 219 (1994) 134.
[18] P.J. Flory, Trans. Faraday Soc., 51 (1955) 848.
[19] T.G. Scholte, N.L.J. Meijerink, H.M. Schoffeleers and A.M.G. Brands, J. Appl. Polym. Sci., 29 (1984) 3763.
[20] E.T. Hsieh and J.C. Randall, Macromolecules, 15 (1982) 353
[21] B. Wunderlich, Macromolecular Physics; Crystal Melting, Vol. 3, Academic Press, New York, 1980, p. 31–32.
[22] L. Wild, T.R. Ryle, D.C. Knobeloch and I.R. Peat, J. Polym. Sci.: Part B: Polym. Phys., 20 (1982) 441.
[23] Y.V. Kissin, Makromol. Chem., Macromol. Symp., 66 (1993) 83.